Value of PET/MRI for assessing tumor resectability in NSCLC-intra-individual comparison with PET/CT

Messerli, Michael ; de Galiza Barbosa, Felipe ; Marcon, Magda ; Muehlematter, Urs J ; Stolzmann, Paul ; Warschkow, René ; Delso, Gaspar ; Ter Voert, Edwin Egw ; Huellner, Martin W ; Frauenfelder, Thomas ; Veit-Haibach, Patrick

Abstract: OBJECTIVE: The purpose of this study was to compare the diagnostic accuracy of positron emission tomography (PET)/MRI with PET/CT for determining tumor resectability of non-small cell lung cancer (NSCLC). METHODS: Sequential trimodality PET/CT/MRI was performed in 36 patients referred with the clinical question of resectability assessment in NSCLC. PET/CT and PET/MR images including T weighted sequence (T-Dixon) and respiration gated T weighted sequence (T-Propeller) were evaluated for resectability-defining factors; i.e. longest diameter of the tumor, minimal tumor distance to the carina, mediastinal invasion, invasion of the carina, pleural infiltration, pericardial infiltration, diaphragm infiltration, presence of additional nodules. RESULTS: There was no significant difference of maximal axial diameter measurements of the primary lung tumors and narrow limits of agreement in Bland-Altman analysis ranging from -11.1 mm to + 11.8 mm for T-Propeller and from -14.3 mm to + 13.8 mm for T-Dixon sequence. A high agreement of PET/MR with PET/CT for the different resectability-defining factors was observed (k from 0.769 to 1.000). There was an excellent agreement of T-Propeller sequence and CT for additional pulmonary nodule detection (k of 0.829 and 0.833), but only a moderate and good agreement using T-Dixon sequence (k of 0.484 and 0.722). CONCLUSION: In NSCLC the use of PET/MRI, including a dedicated pulmonary MR imaging protocol, provides a comparable diagnostic value for determination of tumor resectability compared to PET/CT. ADVANCES IN KNOWLEDGE: Our findings suggest that whole body PET/MRI can safely be used for the local staging of NSCLC patients. Further studies are warranted to determine whether it is feasible to integrate an imaging sequence in a whole body PET/MRI setting with the potential advantage of detection of liver or brain metastases.

DOI: https://doi.org/10.1259/bjr.20180379

BJR

https://doi.org/10.1259/bjr.20180379

Received: 01 May 2018 | Revised: 22 August 2018 | Accepted: 05 September 2018

Cite this article as:
Messerli M, de Galiza Barbosa F, Marcon M, Muehlematter UJ, Stolzmann P, Warschkow R, et al. Value of PET/MRI for assessing tumor resectability in NSCLC—intra-individual comparison with PET/CT. *Br J Radiol* 2018; **91**: 20180379.

FULL PAPER

Value of PET/MRI for assessing tumor resectability in NSCLC—intra-individual comparison with PET/CT

[1]MICHAEL MESSERLI, MD, [1]FELIPE DE GALIZA BARBOSA, MD, [2]MAGDA MARCON, MD, [1,2]URS J MUEHLEMATTER, MD, [1]PAUL STOLZMANN, MD, [3]RENÉ WARSCHKOW, MD, [4]GASPAR DELSO, PhD, [1]EDWIN EGW TER VOERT, PhD, [1]MARTIN W HUELLNER, MD, [2]THOMAS FRAUENFELDER, MD and [1,5]PATRICK VEIT-HAIBACH, MD

[11]Department of Nuclear Medicine, University Hospital Zurich/University of Zurich, Zurich, Switzerland
[2]Institute of Diagnostic and Interventional Radiology, University Hospital Zurich/University Zurich, Zurich, Switzerland
[33]Departmentof Surgery, Cantonal Hospital St. Gallen, St. Gallen, Switzerland
[4]GE Healthcare, Waukesha, WI, USA
[5]Joint Department Medical Imaging, University Health Network, University of Toronto, Toronto, ON, Canada

Address correspondence to: Dr. Michael Messerli
E-mail: *michael.messerli@usz.ch*

Objective: The purpose of this study was to compare the diagnostic accuracy of positron emission tomography (PET)/MRI with PET/CT for determining tumor resectability of non-small cell lung cancer (NSCLC).
Methods: Sequential trimodality PET/CT/MRI was performed in 36 patients referred with the clinical question of resectability assessment in NSCLC. PET/CT and PET/MR images including T_1 weighted sequence (T_1-Dixon) and respiration gated T_2 weighted sequence (T_2-Propeller) were evaluated for resectability-defining factors; *i.e.* longest diameter of the tumor, minimal tumor distance to the carina, mediastinal invasion, invasion of the carina, pleural infiltration, pericardial infiltration, diaphragm infiltration, presence of additional nodules.
Results: There was no significant difference of maximal axial diameter measurements of the primary lung tumors and narrow limits of agreement in Bland–Altman analysis ranging from −11.1 mm to + 11.8 mm for T_2-Propeller and from −14.3 mm to + 13.8 mm for T_1-Dixon sequence. A high agreement of PET/MR with PET/CT for the different resectability-defining factors was observed (k from 0.769 to 1.000). There was an excellent agreement of T_2-Propeller sequence and CT for additional pulmonary nodule detection (k of 0.829 and 0.833), but only a moderate and good agreement using T_1-Dixon sequence (k of 0.484 and 0.722).
Conclusion: In NSCLC the use of PET/MRI, including a dedicated pulmonary MR imaging protocol, provides a comparable diagnostic value for determination of tumor resectability compared to PET/CT.
Advances in knowledge: Our findings suggest that whole body PET/MRI can safely be used for the local staging of NSCLC patients. Further studies are warranted to determine whether it is feasible to integrate an imaging sequence in a whole body PET/MRI setting with the potential advantage of detection of liver or brain metastases.

INTRODUCTION

Non-small cell lung cancer (NSCLC) is still a main contributor to the global cancer mortality burden.[1] A total of 234,030 new cases are estimated to occur in 2018 only in the USA.[2] While for most malignancies a steady increase of survival was seen in recent years this is almost not the case for lung cancers.[3] In recent years, there were made advances concerning treatment of late staged NSCLC by targeting therapy against the driver mutations of this disease (*e.g.* EGFR, ALK, ROS) with specific immunotherapy.[4,5] Nevertheless, tumor resection was proven to be highly effective and might allow for a curative result in early stages.[6] Imaging plays a key role for the exact evaluation of local tumor extension (T-stage) and assessment of local and distant spread.[7] Especially ^{18}F-fluodeoxyglucose positron emission tomography (^{18}F-FDG PET/CT) was proven to be an important tool for assessing lymph node (N) and distant metastasis (M) in patients with NSCLC[8] and is therefore implemented in various international guidelines for presurgical evaluation.[9]

PET/MRI is a relatively new modality that came into clinical use only a few years ago.[10] While initially the use of MRI for chest imaging was perceived as a challenging topic,[11] recent studies indicated that PET/MRI in NSCLC might be non-inferior for early tumor stages[12,13] and possibly even superior compared to PET/CT with regard to lesion conspicuity and/or diagnostic confidence in advanced stages with

liver or bone lesions.[14,15] Further, PET/MR might be beneficial for detecting brain metastases.[16]

Therefore, the purpose of the present study was to test whether ^{18}F-FDG PET/MRI, including a dedicated but short pulmonary MRI protocol, provides an equivalent diagnostic value for determining tumor resectability compared to the present standard of care with ^{18}F-FDG PET/CT in NSCLC patients.

METHODS AND MATERIALS

This study was performed in subjects enroled in a prospective single-center trial. Patients were acquired prospectively as part of a larger prospective study with several different subgroups. The study was approved by the local ethics committee and written informed consent was obtained from all study subjects prior to the examination.

Patients

A total of 45 consecutive adult patients (median age 64 years, range 39–85 years; 16 female and 29 male) referred for either staging (n = 34) or restaging/follow up (n = 11) of suspected or known NSCLC participated in this study. All patients were referred with the clinical question for resectability assessment. Inclusion criteria were (a) clinically indicated ^{18}F-FDG PET/CT and (b) willingness to participate in an additional MRI examination. Exclusion criteria were (a) unwillingness to undergo an additional MRI examination, and (b) contraindications for MRI (*e.g.* claustrophobia, MR-incompatible implanted medical devices). Of the 45 patients initially included, 9 patients were subsequently excluded due to histological results other than NSCLC (small cell lung cancer, n = 3; metastases of cervical cancer, n = 1; neuroendocrine tumor, n = 1; inflammatory disease n = 1) or because no lung lesion was detected (n = 3). Finally, 36 patients were left for evaluation (median age 64, range 44–85 years; 11 female and 25 male).

Imaging techniques

Imaging was performed on a sequential trimodality PET/CT/MRI set-up. The system consists of a full-ring time-of-flight 64-slice PET/CT scanner (Discovery PET/CT 690 VCT, GE Healthcare, Waukesha, WI) and a 3-Tesla (3T) MR scanner (Discovery MR 750w, GE Healthcare, Waukesha, WI), connected by a shuttle device that allows for sequential scanning without repositioning of the patient.[17]

Table 1. Acquisition parameters of MRI pulse sequences

	T_2-Propeller	T_1-Dixon
Repetition time/echo time, ms*	~10000/100	4.3/1.6
Slice thickness, mm	4.5	4.0
Gap, %	2	0
Matrix	288 × 288	288 × 224
Field of view, mm	40	50
Bandwidth, kHz	62.5	142.86
Voxel size, mm^3	1.4 × 1.4×4.5	1.7 × 2.2×2.0
Flip angle°	NA	12
Acquisition time, min:s	~5 min[a]	00:14

[a]The acquisition time of T_2-Propeller depends on the breathing pattern of the patient.

The study patients fasted for at least 4 h before being injected with 250–380 MBq of ^{18}F-FDG depending on the BMI. The total uptake time was set to 60 min. 35–40 min after injection, patients were positioned in the MR scanner. All MR images were acquired during this 20–25 min prior to PET/CT imaging. Whole-body multisection MRI was performed with an axial T_1 weighted three-dimensional dual-echo fast spoiled gradient echo sequence (Liver accelerated volume acquisition, LAVA-Flex). Water-only and fat-only images were automatically generated from the dual-echo acquisition using a Dixon-based method.[18] Further, a T_2 weighted sequence with motion correction (periodically rotated overlapping parallel lines with enhanced reconstruction, PROPELLER) was acquired during free breathing with respiratory triggering.[19] Details on MR acquisition parameters are given in Table 1 and were published previously.[20] No contrast media was administered to the patients for the MR acquisition. Subsequently patients were transferred to the PET/CT, where standard, clinical image acquisition started immediately. The PET data sets covered the region from the vertex of the skull to the mid thighs. Low dose CT covering the same region as PET, used for attenuation correction purposes as well as for anatomic

Table 2. Imaging criteria for potential tumor resectability as assessed by the readers

		Resectable	Unresectable
Local tumor assessment	Tumor size	Tumor <7 cm longest diameter	Tumor >7 cm longest diameter
	Distance to carina	Tumor distance to carina >2 cm	Tumor distance to carina <2 cm
	Mediastinal infiltration	No mediastinal infiltration	Mediastinal infiltration
	Pleural infiltration	No pleural or only visceral pleural infiltration	Parietal pleural infiltration
	Pericardium infiltration	Pericardium not infiltrated	Pericardium infiltrated
	Diaphragm infiltration	No infiltration of the diaphragm	Infiltration of the diaphragm
	Infiltration of the brachial plexus	Brachial plexus not infiltrated	Brachial plexus infiltrated
	Infiltration of the fissure / lobe	No infiltration of the fissure and adjacent lobe	Infiltration of the fissure and adjacent lobe
Lung nodules	Additional lung nodules	No additional nodules or only in ipsilateral lobes	Separate nodules in a contralateral lobe

Table 3. TNM-status[a] of 36 patients

	n (%)
T-Stage	
T1	11 (31 %)
T2	7 (19 %)
T3	12 (33 %)
T4	6 (17 %)
N-Stage	
N0	12 (34 %)
N1	8 (22 %)
N2	9 (25 %)
N3	7 (19 %)
M-Stage	
M0	29 (81 %)
M1	7 (19 %)

[a]Final stages were assessed by histopathological (n = 19) and clinical (n = 17) follow-up.

localization of ^{18}F-FDG uptake was acquired. Further, a regular dose CT scans of the chest was acquired in breath-hold as by clinical standard in patients referred for staging/restaging of lung cancer. After the acquisition of the PET data, 70 ml of intravenous contrast (Visipaque 320, GE Healthcare, Waukesha, WI) were injected with a flow rate of 3 ml s^{-1}. The CT scan was started 60 s after initiating the contrast injection. Scan parameters were as follows: Tube voltage, 100 kV; tube current with automated dose modulation, 60–440 mA/slice; pitch 0.984:1; collimation 64 × 0.625; rotation time, 0.5 s; coverage speed 78 mm/s; field of view 40 cm; images with a transverse pixel size of 0.625 mm and a slice thickness of 2.5 mm, reconstructed in the axial, sagittal and coronal plane with 1.25 mm. The entire PET/CT-MR acquisition protocol imaging setup has been published several times for different research questions by our group before.[21]

Imaging processing and reading technique

Analyses of the acquired PET, CT and MR image data sets were carried out on a dedicated review workstation (Advantage Workstation, v. 4.6, GE Healthcare, Waukesha, WI), which allows for viewing images of all modalities side-by-side and/or overlay mode (CT, PET as well as PET/CT and PET/MR). Only combined PET/CT images and PET/MR images were compared for this study as done before in other tri-modality studies from our group.[21] For our study, the T_1 weighted sequence water-only (*i.e.* LAVA-Flex in breath-hold, hereafter called T_1-Dixon) and the respiration gated T_2 weighted (*i.e.* Propeller, hereafter called T_2-Propeller) were assessed.

Data analyses

Two radiologists (Ma.M. and T.F., with 5 and 14 years of experience in chest radiology) assessed anonymized image data sets in random order and blinded to all clinical information, except the fact of suspected or known presence of NSCLC. Both readers interpreted PET/CT images first, followed by PET/MR images with a delay of 6 weeks between the readings in order minimize the potential of recall bias. On PET/CT and PET/MRI, the readers assessed pre-defined factors concerning local tumor resectability. These factors included six findings determining T-classification of the tumor (*i.e.* mediastinal infiltration, visceral or parietal pleural infiltration, infiltration of the pericardium, infiltration of the diaphragm, infiltration of the brachial plexus, infiltration of the fissure/adjacent lobe), and another three criteria that are taken into consideration for local tumor stage assessment (longest diameter of the tumor, distance to carina, presence of additional nodules). The longest/maximal diameter of the tumor was measured in the axial plane where the largest tumor extent was seen in CT and MR For the measurement in CT lung window settings were used. Table 2 summarizes the imaging criteria to determine the resectability as assessed by the readers and as previously suggested.[22]

Statistical analyses

All statistical analyses were performed using SPSS 23.0 (IBM Corporation, Armonk, NY) and MedCalc v. 15.8 (MedCalc

Figure 1. Bland–Altman plot for measurement of tumor diameter in all patients (n = 36) in CT images and MR T_2-Propeller images (A), and MR T_1-Dixon (B) displaying the measurements of both readers. Bland-Altman limits of agreement were −11.1 to 11.8 mm comparing MR T_2-Propeller with CT with a mean difference of +0.35 mm (A) and −14.3 to 13.8 mm comparing MR T_1-Dixon with CT with a mean difference of −0.27 mm (B), both $p > 0.05$.

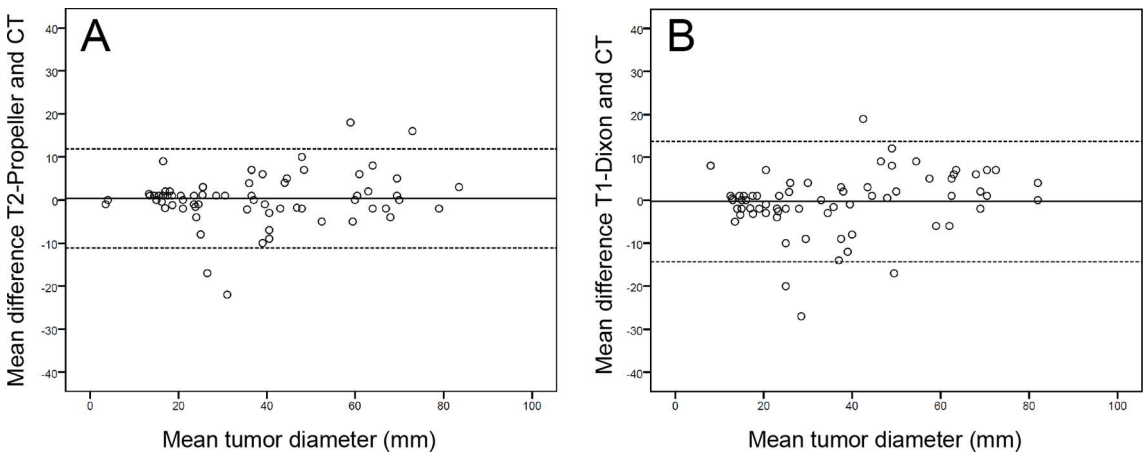

Figure 2. BlandAltman plot for measurements of the distance of the tumor from the carina in CT images and MR T_2-Propeller images (A), and MR T_1-Dixon (B) in patients with tumors located <5 cm to the carina but without reaching the carina. Measurements of both readers are displayed. Bland-Altman limits of agreement were −6.0 to 11.5 mm comparing MR T_2-Propeller with CT with a mean difference of +2.8 mm (A), $p < 0.05$. Limits of agreement comparing MR T_1-Dixon with CT were −8.6 to 12.2 mm with a mean difference of +1.8 mm (B), $p > 0.05$.

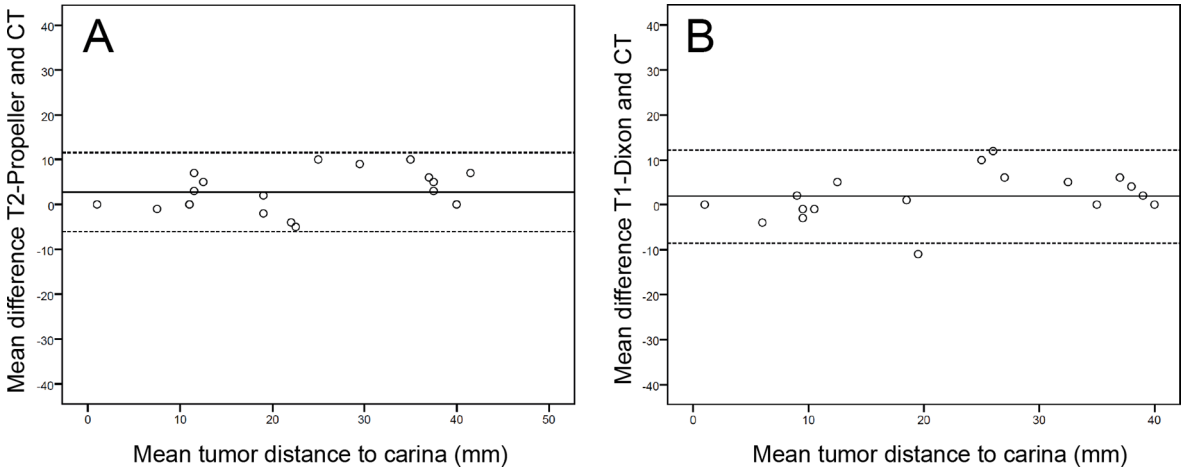

Software, Ostend, Belgium). Categorical variables are expressed as proportions, and continuous variables are presented as mean ± standard deviation or median (range) depending on the distribution of values. A two-tailed p-value of <0.05 was considered to indicate significance for all statistical tests applied.

Comparison of tumor diameters and distance to the carina in CT and MR

To evaluate agreement of tumor measurements in CT and MR scans, differences of size were plotted against the mean diameter using the Bland–Altman method. The limits of agreement were defined as the mean difference ±1.96 × standard deviation. Bland–Altman analyses including the measurements of both readers were performed (a) for primary lung tumors and (b) for tumor distance to the carina for all patients where primary tumor was localized >0 cm to <5 cm. Further, differences of tumor measurements and measurements of tumor distance to the carina among CT and MR were statistically compared using a one-sided t-test against zero.

Assessment of agreement of tumor distance to the Carina and resectability-defining factors

The agreement of whether a tumor was >2 cm from,>0–2 cm from, or abutting/invading the carina as well as all resectability-defining factor between CT and MR sequences for both readers and the readers separately was determined using linear weighted kappa statistics, with 95% confidence intervals (CIs). The k values were interpreted as: poor ($k < 0.20$), fair ($k = 0.21$–0.40), moderate ($k = 0.41$–0.60), good ($k = 0.61$–0.80), and excellent ($k = 0.81$–1.00) agreement.[23]

Assessment of potential resectability

Based on local tumor extent of CT and MR, the potential resectability of the NSCLC was defined, according the factors listed

Table 4. Reader agreement of CT and MR images for resectability-defining factors for the study patients ($n = 36$)

		PET/CT *vs* PET/MR T_2 Propeller			PET/CT *vs* PET/MR T_2 Dixon		
		Overall	Reader 1	Reader 2	Overall	Reader 1	Reader 2
Local tumor assessment[a]	Mediastinal infiltration	0.968 (0.907–1.000)	0.936 (0.813–1.000)	1.000 (1.000–1.000)	0.968 (0.907–1.000)	0.936 (0.813–1.000)	1.000 (1.000–1.000)
	Pleural infiltration	1.000 (1.000–1.000)	1.000 (1.000–1.000)	1.000 (1.000–1.000)	0.881 (0.783–0.979)	0.804 (0.638–0.970)	0.953 (0.862–1.000)
	Diaphragm infiltration	1.000 (1.000–1.000)	1.000 (1.000–1.000)	1.000 (1.000–1.000)	1.000 (1.000–1.000)	1.000 (1.000–1.000)	1.000 (1.000–1.000)
	Infiltration of the fissure/lobe	0.820 (0.683–0.957)	0.875 (0.707–1.000)	0.769 (0.562–0.977)	0.791 (0.645–0.937)	0.816 (0.618–1.000)	0.769 (0.562–0.977)
Lung nodules	Additional lung nodules	0.829 (0.698–0.960)	0.822 (0.630–1.000)	0.833 (0.655–1.000)	0.618 (0.438–0.799)	0.484 (0.185–0.783)	0.722 (0.505–0.939)

*k*of pairwise comparisons overall as well as for both readers separately aredisplayed, 95% confidence interval inparenthesis.
[a]Results for pericardial infiltration ($n = 0$), and brachial plexus invasion ($n = 0$) are not shown in the table because of the low prevalence in the study patients.

Figure 3. Sankey plots illustrating ratings of resectability-defining factors comparing PET/MR sequences with CT including the ratings of both readers. PET, positron emission tomography.

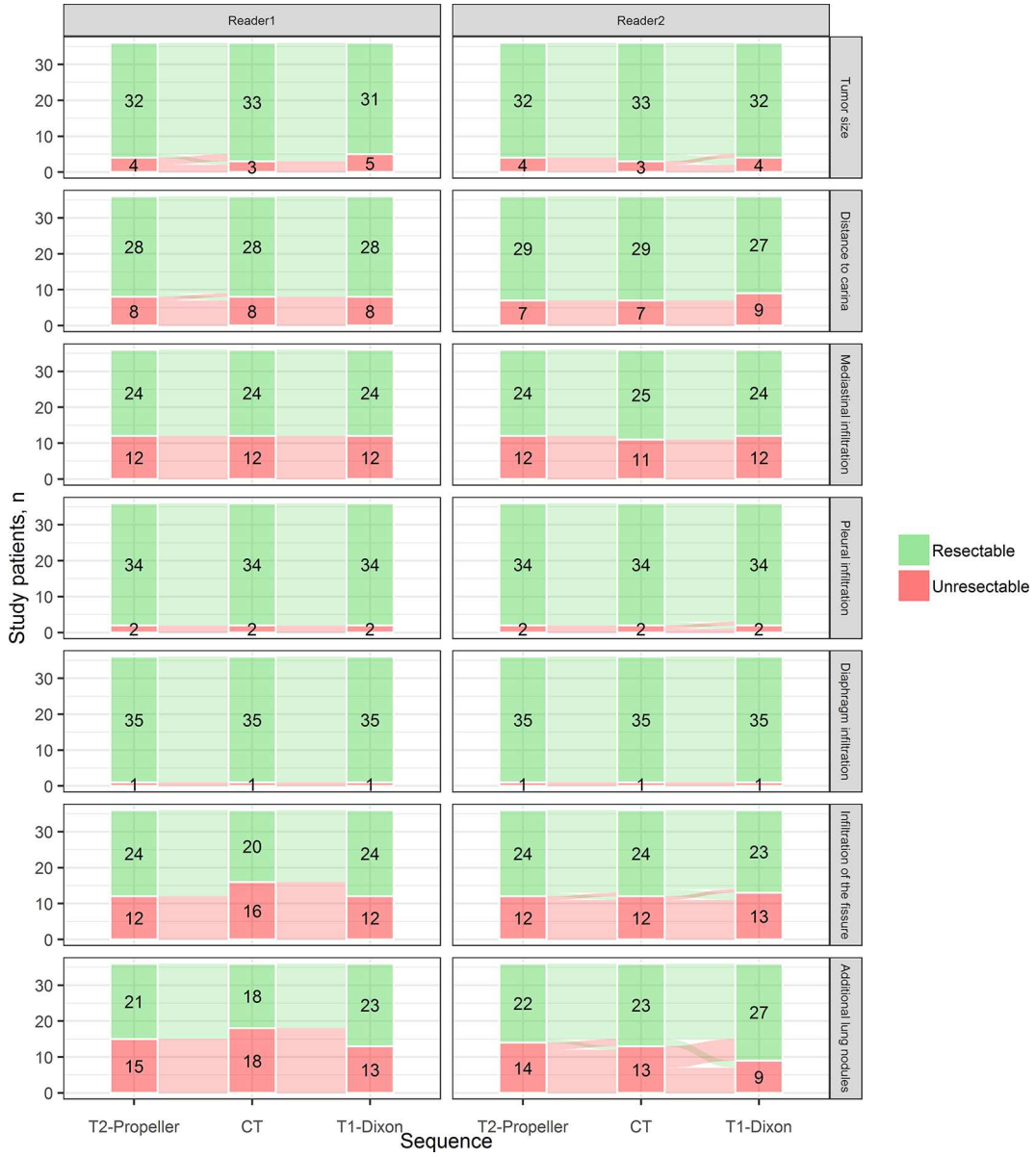

in Table 2. A score of 1 was assigned if the PET/MR assessment revealed a resectable tumor and a score of 0 if the tumor was not resectable, with PET/CT serving as standard of reference.

RESULTS

The final TNM classification of the included 36 patients is presented in Table 3.

Assessment of tumor size in CT and MR

The mean tumor size was 36.5 ± 19.7 mm on CT, and 36.9 ± 20.7 mm on PET/MR T_2-Propeller and 36.3 ± 21.1 mm on T_1-Dixon, respectively. Bland–Altman analysis comparing PET/MR T_2-Propeller with PET/CT revealed a mean difference of +0.3 mm and limits of agreement from −11.1 to 11.8 mm, the mean difference thereby was not statistically different (p = 0.62). Similarly, comparing PET/MR T_1-Dixon with PET/CT we observed a mean difference of −0.3 mm and limits of agreement of −14.3 to 13.8 mm, the mean difference was not statistically different (p = 0.75). Bland-Altman plots are shown in Figure 1.

Measurement of distance to Carina in PET/CT and PET/MR

The mean distance of lung tumor to the carina was 22.2 ± 12.3 mm on CT, and 25.0 ± 13.7 mm on PET/MR T_2-Propeller and 22.9 ± 14.1 mm on T_1-Dixon, respectively. The Bland–Altman plots for measurements of the tumor distance to the carina are given in Figure 2. Bland–Altman analysis comparing PET/MR T_2-Propeller with PET/CT revealed a mean difference of +2.8 mm and limits of agreement from −6.0 to 11.5 mm, the mean difference thereby was statistically different (p = 0.01). Comparing PET/MR T_1-Dixon with PET/CT, we observed a mean difference of +1.8

Figure 4. Sankey plots illustrating per patient analyses for lung tumor resectability comparing PET/MR sequences with CT including the ratings of both readers. PET, positron emission tomography.

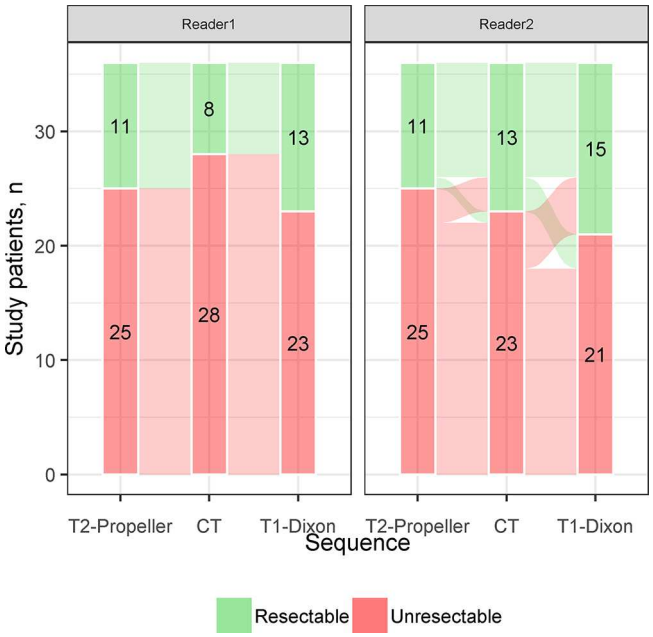

mm and limits of agreement from −8.6 to 12.2 mm, the mean difference was not statistically different ($p = 0.16$).

κ statistics showed a high agreement of T_2-Propeller and CT images on whether the distance of the tumor was >2 cm from the carina,>0 – 2 cm from from the carina, or abutting/invading the carina for with a weighted kappa of 0.888 [95% CI (0.789–0.987)]. There was also a high agreement of T_1-Dixon and CT on the same subject with a weighted κ of 0.808 [95% CI (0.663 – 0.953)], $p < 0.001$.

Diagnostic agreement of resectability-defining factors of PET/MR compared to PET/CT

There was generally a high agreement for most resectability-defining factors, with mostly *k*-values indicating excellent agreement. Detailed data including all *k*-values for the assessment of resectability-defining factors comparing CT and MR are given in Table 4.

Analysis for potential resectability

Differences of resectability-defining factors as assessed by MR and CT by both readers are presented in Figure 3. Of all 36 subjects, 33 (92%) and 32 (89%) were correctly classified by T_2-Propeller by Reader 1 and Reader 2 using CT as reference, respectively, Figure 4. Of all 36 subjects, 31 (86%) and 28 (78%) were correctly classified by T_1-Dixon by Reader 1 and Reader 2 using CT as reference, respectively, see Figure 4. Representative images of PET/CT and PET/MR are given in Figure 5.

DISCUSSION

This study sought to determine the accuracy of ^{18}F-FDG PET/MRI for assessing tumor resectability in NSCLC. We therefore prospectively included patients undergoing clinically indicated PET/CT for lung cancer resectability assessment and imaged them with MR using a respiration-gated T_2 weighted sequence and three-dimensional dual-echo GRE pulse sequence in a trimodality PET/CT-MR setup. We found a high agreement of different resectability defining factors of PET/MR with PET/CT as reference among readers with different levels of experience.

PET/CT has proven to be a vital tool for a thorough assessment of patients with NSCLC because of the high spatial resolution of CT and the additional metabolic information derived by the ^{18}F-FDG PET for detection of lymph nodes and distant metastasis.[24–26] Optimal staging is particularly important in a presurgical stage to limit surgery or multimodality treatment to only those patients who might benefit from such a therapy and avoid potentially futile surgery, related morbidity as well as unnecessary costs.

When comparing PET/MR with the reference PET/CT we found no significant difference of maximal axial diameter measurements of the primary lung tumors and narrow limits of agreement in Bland–Altman analysis ranging from −11.1 mm to +11.8 mm for T_2-Propeller and from −14.3 mm to +13.8 mm for T_1-Dixon sequence, respectively. This is in line with a previous study that reported excellent agreement for estimation of the size of primary tumors in PET/MR.[12] A reliable estimation of the maximal axial diameter of lung tumors in different imaging modalities is important, as this measure reflects the pathological T-stage.[27] It has to be pointed out that our protocol was acquired without contrast media and with basically only two sequences. The reason for that was to test whether a fast and rather basic protocol for the lung is sufficient for diagnostic purposes since the MRI–component within a PET/MR is often very lengthy. Thus, in view of testing an MRI protocol for possible integration into a whole-body PET/MRI, only this limited protocol was chosen. We would also like to highlight that given the recent technical improvement of MR sequences we were able to perform respiration-gated MR scans at reasonably low scanning times.

A previous study reported some source of bias owing to potential misinterpretation of main bronchus involvement in PET/MR.[28] In contradiction to that, we found an overall excellent agreement for the classification of tumor distance to the carina for T_2-Propeller and T_1-Dixon, respectively. Interestingly, there was a tendency for overestimating the tumor distance to carina in T_2-Propeller sequence, however even though this was statistically significant, this is most likely not clinically relevant with a mean difference (*i.e.* overestimation) of measurement of only +2.8 mm. Moreover, as stated before the agreement on whether a tumor was >2 cm from,>0–2 cm from, or abutting/invading the carina was excellent comparing T_2-Propeller with CT.

Our study is one of the early evaluations to investigate the relevant resectability defining factors instead of comparing T-stages in simultaneous PET/CT and PET/MR. By doing that, we observed a good to excellent agreement of MR with CT for mediastinal infiltration, pleural infiltration, infiltration of diaphragm and adjacent lobe. Despite the aforementioned

Figure 5. Representative images of a 62-year-old female that underwent sequential trimodality PET/CT/MRI referred for resectability assessment of NSCLC. Coronal PET maximum-intensity-projection image (A) shows a focal FDG-active lesion in the left upper lobe (arrow). Axial CT image (B) shows a nodule in the left upper lobe and axial coregistered PET/CT image (C) confirms 18F-FDG-activity of the lesion. MR and PET/MR images with T_2-Propeller (D, E) as well as T_1-Dixon (F, G). The readers independently agreed on PET/CT as well as PET/MR on resectability of the tumor. The patient subsequently underwent lobectomy and final histopathological diagnosis confirmed adenocarcinoma. 18F-FDG, 18F-fluodeoxyglucose; NSCLC, non-small cell lung cancer; PET, positron emission tomography.

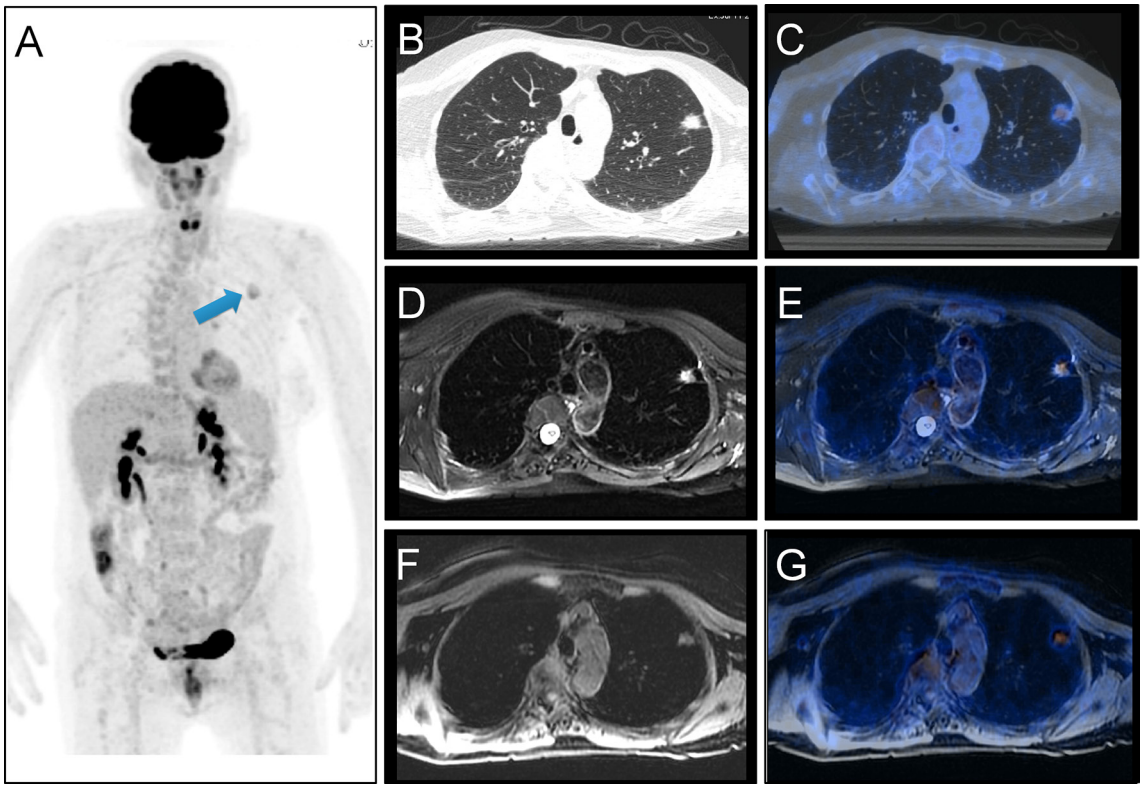

efforts and results, one of the concerns for substituting the CT component in PET/CT with the MR component in PET/MR is the lower accuracy or even described inability of MRI for the detection of small lung nodules.[29–31] However, we observed an excellent agreement of T_2-Propeller sequence with CT for nodule detection with κ values of 0.829 and 0.833 of the two readers, but only a moderate and good agreement using T_1-Dixon sequence with a κ of 0.484 and 0.722 of the two readers. Previous reports also presented similar data with T_2-Propeller yielding significantly higher nodule detection rates than Dixon MR in oncological patients, including a subanalysis for PET-positive as well as confirmed malignant nodules.[32] Also in the latter categories, the T_2-Propeller was not significantly inferior compared to CT from PET/CT. However, concerning overall detection rates of lung lesions, the MRI from PET/MR was still inferior compared to CT with significantly lower detection rates for small lesions. Thus, for staging purposes with known lung lesions, PET/MR might be safely used but it is certainly still not comparable to CT for smaller pulmonary lesions.

Additional improvements of MR sequences for lung imaging are on the horizon—with the most promising probably being short echo time imaging (*e.g.* ultra-short time to echo and zero time to echo—so called UTE- and ZTE-sequences). Recently, Ohno et al demonstrated improved pulmonary nodule detection rates of thin-section MRI with UTE and further described the usefulness of UTE for evaluation of nodule type as at least as efficacious as standard-dose thin-section CT.[33] Other studies using UTE-sequences have shown a good visualization of the lung parenchyma and mediastinum in adult patients[34,35] as well as a good visibility of the airways including the trachea and main bronchi in infants.[36]

There are several limitations that have to be considered in the present study. There are only a limited number of patients included in this study which is why our results must be regarded as initial results with the introduced sequences and any conclusions drawn from the present analysis awaits further proof in bigger (ideally multicentric) observations. As a result of the low number of patients, we encountered a second limitation which includes the fact that not all primarily intended resectability defining factors occurred in the study group such as brachial plexus infiltration.

In conclusion, we found that PET/MRI, including a dedicated but short pulmonary MRI protocol, provides a comparable diagnostic value for determination of tumor resectability compared to PET/CT. Further studies are warranted to determine whether

it is feasible to integrate whole body PET/MRI in NSCLC staging with potential advantages for detection of liver or brain metastases.

ACKNOWLEDGMENT

Michael Messerli received a research grant from the Iten-Kohaut Foundation, Switzerland. The authors want to thank Marlena Hofbauer, Sabrina Epp, Miguel Porto and Sofia Kaltsuni for their excellent technical support.

CONFLICT OF INTEREST

Patrick Veit-Haibach received investigator-initiated study grants from Bayer Healthcare, GE Healthcare and Roche Pharmaceuticals, and speaker fees from GE Healthcare. Gaspar Delso is an employee of GE Healthcare. Martin Huellner received speaker's fees from GE Healthcare. The other authors of this manuscript declare no relationships with any companies, whose products or services may be related to the subject matter of the article. There was financial support for this study from GE Healthcare on an institutional level. Only non-GE Healthcare employees had control of inclusion of the data and information that might present a conflict of interest for those authors who are employees of GE Healthcare.

REFERENCES

1. Stewart B, Wild C. World cancer report 2012. *International Agency for Research on Cancer* 2014;.
2. Siegel RL, Miller KD, Jemal A. Cancer statistics. *CA Cancer J Clin* 2018; **2018**.
3. Siegel RL, Miller KD, Jemal A. Cancer Statistics, 2017. *CA Cancer J Clin* 2017; **67**: 7–30. doi: https://doi.org/10.3322/caac.21387
4. Novello S, Barlesi F, Califano R, Cufer T, Ekman S, Levra MG, et al. Metastatic non-small-cell lung cancer: ESMO Clinical Practice Guidelines for diagnosis, treatment and follow-up. *Ann Oncol* 2016; **27**(suppl 5): v1–v27. doi: https://doi.org/10.1093/annonc/mdw326
5. Recondo G, Facchinetti F, Olaussen KA, Besse B, Friboulet L. Making the first move in EGFR-driven or ALK-driven NSCLC: first-generation or next-generation TKI? *Nat Rev Clin Oncol* 2018;. doi: https://doi.org/10.1038/s41571-018-0081-4
6. Howington JA, Blum MG, Chang AC, Balekian AA, Murthy SC. Treatment of stage I and II non-small cell lung cancer: Diagnosis and management of lung cancer, 3rd ed: American College of Chest Physicians evidence-based clinical practice guidelines. *Chest* 2013; **143**(5 Suppl): e278S–e313S. doi: https://doi.org/10.1378/chest.12-2359
7. Lardinois D, Weder W, Hany TF, Kamel EM, Korom S, Seifert B, et al. Staging of non-small-cell lung cancer with integrated positron-emission tomography and computed tomography. *N Engl J Med* 2003; **348**: 2500–7. doi: https://doi.org/10.1056/NEJMoa022136
8. Pieterman RM, van Putten JW, Meuzelaar JJ, Mooyaart EL, Vaalburg W, Koëter GH, et al. Preoperative staging of non-small-cell lung cancer with positron-emission tomography. *N Engl J Med* 2000; **343**: 254–61. doi: https://doi.org/10.1056/NEJM200007273430404
9. Silvestri GA, Gonzalez AV, Jantz MA, Margolis ML, Gould MK, Tanoue LT, et al. Methods for staging non-small cell lung cancer: Diagnosis and management of lung cancer, 3rd ed: American College of Chest Physicians evidence-based clinical practice guidelines. *Chest* 2013; **143**(5 Suppl): e211S–e250S. doi: https://doi.org/10.1378/chest.12-2355
10. Drzezga A, Souvatzoglou M, Eiber M, Beer AJ, Fürst S, Martinez-Möller A, et al. First clinical experience with integrated whole-body PET/MR: comparison to PET/CT in patients with oncologic diagnoses. *J Nucl Med* 2012; **53**: 845–55. doi: https://doi.org/10.2967/jnumed.111.098608
11. Ohno Y. New applications of magnetic resonance imaging for thoracic oncology. *Semin Respir Crit Care Med* 2014; **35**: 027–40. doi: https://doi.org/10.1055/s-0033-1363449
12. Heusch P, Buchbender C, Köhler J, Nensa F, Gauler T, Gomez B, et al. Thoracic staging in lung cancer: prospective comparison of 18F-FDG PET/MR imaging and 18F-FDG PET/CT. *J Nucl Med* 2014; **55**: 373–8. doi: https://doi.org/10.2967/jnumed.113.129825
13. Schwenzer NF, Schraml C, Müller M, Brendle C, Sauter A, Spengler W, et al. Pulmonary lesion assessment: comparison of whole-body hybrid MR/PET and PET/CT imaging--pilot study. *Radiology* 2012; **264**: 551–8. doi: https://doi.org/10.1148/radiol.12111942
14. Beiderwellen K, Huebner M, Heusch P, Grueneisen J, Ruhlmann V, Nensa F, et al. Whole-body [^{18}F]FDG PET/MRI vs. PET/CT in the assessment of bone lesions in oncological patients: initial results. *Eur Radiol* 2014; **24**: 2023–30. doi: https://doi.org/10.1007/s00330-014-3229-3
15. Beiderwellen K, Gomez B, Buchbender C, Hartung V, Poeppel TD, Nensa F, et al. Depiction and characterization of liver lesions in whole body [^{18}F]-FDG PET/MRI. *Eur J Radiol* 2013; **82**: e669–e675. doi: https://doi.org/10.1016/j.ejrad.2013.07.027
16. Yi CA, Shin KM, Lee KS, Kim BT, Kim H, Kwon OJ, et al. Non-small cell lung cancer staging: efficacy comparison of integrated PET/CT versus 3.0-T whole-body MR imaging. *Radiology* 2008; **248**: 632–42. doi: https://doi.org/10.1148/radiol.2482071822
17. Veit-Haibach P, Kuhn FP, Wiesinger F, Delso G, von Schulthess G. PET-MR imaging using a tri-modality PET/CT-MR system with a dedicated shuttle in clinical routine. *MAGMA* 2013; **26**: 25–35. doi: https://doi.org/10.1007/s10334-012-0344-5
18. Ma J. Breath-hold water and fat imaging using a dual-echo two-point Dixon technique with an efficient and robust phase-correction algorithm. *Magn Reson Med* 2004; **52**: 415–9. doi: https://doi.org/10.1002/mrm.20146
19. Pipe JG. Motion correction with PROPELLER MRI: application to head motion and free-breathing cardiac imaging. *Magn Reson Med* 1999; **42**: 963–9. doi: https://doi.org/10.1002/(SICI)1522-2594(199911)42:5<963::AID-MRM17>3.0.CO;2-L
20. Huellner MW, Appenzeller P, Kuhn FP, Husmann L, Pietsch CM, Burger IA, et al. Whole-body nonenhanced PET/MR versus PET/CT in the staging and restaging of cancers: preliminary observations. *Radiology* 2014; **273**: 859–69. doi: https://doi.org/10.1148/radiol.14140090
21. Martini K, Meier A, Opitz I, Weder W, Veit-Haibach P, Stahel RA, et al. Diagnostic accuracy of sequential co-registered PET+MR in comparison to PET/CT in

local thoracic staging of malignant pleural mesothelioma. *Lung Cancer* 2016; **94**: 40–5. doi: https://doi.org/10.1016/j.lungcan.2016.01.017
22. Quint LE. Lung cancer: assessing resectability. *Cancer Imaging* 2003; **4**: 15–18. doi: https://doi.org/10.1102/1470-7330.2003.0028
23. JR L, GG K. A one-way components of variance model for categorical data. *Biometrics* 1977; **33**: 671–9.
24. Antoch G, Stattaus J, Nemat AT, Marnitz S, Beyer T, Kuehl H, et al. Non-small cell lung cancer: dual-modality PET/CT in preoperative staging. *Radiology* 2003; **229**: 526–33. doi: https://doi.org/10.1148/radiol.2292021598
25. Goeckenjan G, Sitter H, Thomas M, Branscheid D, Flentje M, Griesinger F, et al. Prevention, diagnosis, therapy, and follow-up of lung cancer. Interdisciplinary guideline of the German Respiratory Society and the German Cancer Society--abridged version. *Pneumologie* 2011; **65**: e51–75. doi: https://doi.org/10.1055/s-0030-1256562
26. National Collaborating Centre for Cancer U (2011) The diagnosis and treatment of lung cancer (Update. *National Collaborating Centre for Cancer (UK), Cardiff*.
27. Heidinger BH, Anderson KR, Moriarty EM, Costa DB, Gangadharan SP, VanderLaan PA, et al. Size Measurement and T-staging of Lung Adenocarcinomas Manifesting as Solid Nodules ≤30 mm on CT: Radiology-Pathology Correlation. *Acad Radiol* 2017; **24**: 851–9. doi: https://doi.org/10.1016/j.acra.2017.01.009
28. Huellner MW, de Galiza Barbosa F, Husmann L, Pietsch CM, Mader CE, Burger IA, et al. TNM Staging of Non-Small Cell Lung Cancer: Comparison of PET/MR and PET/CT. *J Nucl Med* 2016; **57**: 21–6. doi: https://doi.org/10.2967/jnumed.115.162040
29. Chandarana H, Heacock L, Rakheja R, DeMello LR, Bonavita J, Block TK, et al. Pulmonary nodules in patients with primary malignancy: comparison of hybrid PET/MR and PET/CT imaging. *Radiology* 2013; **268**: 874–81. doi: https://doi.org/10.1148/radiol.13130620
30. Sieren JC, Ohno Y, Koyama H, Sugimura K, McLennan G. Recent technological and application developments in computed tomography and magnetic resonance imaging for improved pulmonary nodule detection and lung cancer staging. *J Magn Reson Imaging* 2010; **32**: 1353–69. doi: https://doi.org/10.1002/jmri.22383
31. Stolzmann P, Veit-Haibach P, Chuck N, Rossi C, Frauenfelder T, Alkadhi H, et al. Detection rate, location, and size of pulmonary nodules in trimodality PET/CT-MR: comparison of low-dose CT and Dixon-based MR imaging. *Invest Radiol* 2013; **48**: 241–6. doi: https://doi.org/10.1097/RLI.0b013e31826f2de9
32. de Galiza Barbosa F, Geismar JH, Delso G, Messerli M, Huellner M, Stolzmann P, et al. Pulmonary nodule detection in oncological patients - Value of respiratory-triggered, periodically rotated overlapping parallel T2-weighted imaging evaluated with PET/CT-MR. *Eur J Radiol* 2018; **98**: 165–70. doi: https://doi.org/10.1016/j.ejrad.2017.11.010
33. Ohno Y, Koyama H, Yoshikawa T, Kishida Y, Seki S, Takenaka D, et al. Standard-, reduced-, and no-dose thin-section radiologic examinations: comparison of capability for nodule detection and nodule type assessment in patients suspected of having pulmonary nodules. *Radiology* 2017; **284**: 562–73. doi: https://doi.org/10.1148/radiol.2017161037
34. Gai ND, Malayeri A, Agarwal H, Evers R, Bluemke D. Evaluation of optimized breath-hold and free-breathing 3D ultrashort echo time contrast agent-free MRI of the human lung. *J Magn Reson Imaging* 2016; **43**: 1230–8. doi: https://doi.org/10.1002/jmri.25073
35. Ohno Y, Koyama H, Yoshikawa T, Seki S, Takenaka D, Yui M, et al. Pulmonary high-resolution ultrashort TE MR imaging: Comparison with thin-section standard- and low-dose computed tomography for the assessment of pulmonary parenchyma diseases. *J Magn Reson Imaging* 2016; **43**: 512–32. doi: https://doi.org/10.1002/jmri.25008
36. Niwa T, Nozawa K, Aida N. Visualization of the airway in infants with MRI using pointwise encoding time reduction with radial acquisition (PETRA. *J Magn Reson Imaging* 2017; **45**: 839–44. doi: https://doi.org/10.1002/jmri.25420